CrossMark

ORIGINAL PAPER

Multiple indicators prediction method of rock burst based on microseismic monitoring technology

Shuren Wang[1,2] · Chunyang Li[2] · Wenfa Yan[3] · Zhengsheng Zou[1] · Wenxue Chen[1,2,4]

Abstract Rock burst prediction method for coal mining is one of the worldwide challenging problems. Based on a high precision microseismic monitoring system consisting of nine geophones installed in Qixing Coal Mine in China, abundant microseismic events were detected through the continuous monitoring for 80 days. The potential high risk areas of rock burst were determined by analyzing the spatial and temporal distribution characteristics of microseismic events, which provides the basis for the early risk warning during the mining process. After a comprehensive analysis of the spatial and temporal evolution characteristics of the microseismic events, a prediction model for rock burst prediction was built based on the principles of seismology and rock mechanics by setting four indicators as prediction parameters, such as the average number of microseismic events N, the average released energy E, the decrease Δb of the seismological parameter b, and the potential maximum seismic magnitude M_{m}. It was found that all the four prediction indicators are useful for predicting rock burst but they could vary greatly in efficiency in the practical engineering applications.

✉ Wenxue Chen
  wen1xue2@126.com

1 Opening Laboratory for Deep Mine Construction, Henan
  Polytechnic University, Jiaozuo 454003, China

2 International Joint Research Laboratory of Henan Province for
  Underground Space Development and Disaster Prevention, Henan
  Polytechnic University, Jiaozuo 454003, China

3 Anhui Wantai Geophysical Technology Co., Ltd, Hefei 230011,
  China

4 Department of Building, Civil and Environmental Engineering,
  Concordia University, Quebec H3G 1M8, Canada

Introduction

Rock burst is one of the most serious geological disasters in the worldwide mining engineering (Jiang et al., 2014). However, it is difficult to be predicted timely because it often occurs without obvious precursors. In recent years, the microseismic monitoring has gradually become an important early warning method for preventing rock burst. Compared with other monitoring methods, it can provide detailed information on potential risks in both space and time domains.

Microseismic monitoring has been tested in forecasting rock burst in various mines. For example, Mansurov (2001) proposed a prediction technique by analyzing microseismic data and this technique showed a high efficiency when it was applied in the retrospect for the induced seismicity database in Bauxite coal mine. Driad-Lebeau et al. (2005) delineated other high risk areas by analyzing the cause and process of a strong rock burst occurred in Frieda 5 coal mine in eastern France. Lesniak and Isakow (2009) analyzed the spatial and temporal characteristics of 2-month microseismic events in Zabrze-Bielszowice coal mine in Poland, and pointed out the relations between the occurrence of rock burst and established a hazard assessment function. Xia et al. (2010) selected five indicators to predict rock burst and discussed their prediction efficiencies respectively. Yuan et al. (2012) and Zhao et al. (2012) found that some significant changes in the microseismic waveforms happened before rock bursts, and they thought these signal characteristics would be useful for the rock burst prediction. Based on the induced seismicity data in the excavation process of Base Gotthard tunnel, Husen et al. (2013) discussed the induced effect of rock bursts caused by

multiple fractures in fault zones and the stress redistribution. Yu et al. (2014) explained the preparation process of rock bursts by the crack extension theory, and revealed the relations between the microseisms and rock bursts. Pastén et al. (2015) analyzed over 50,000 microseismic events recorded in Creighton mine by the fractal geometry method, and they tried to verify the relations between the fractal dimension and the occurrence of large magnitude events. By means of the so-called 3S principle in seismology, Ma et al. (2016) proposed four rock burst criterions based on the distribution of the microseismic events in the process of rock damage.

Because the mechanism of rock burst is very complex and each mine has its own characteristics, rock burst prediction is a challenging problem and it still lacks a general prediction method applicable in various cases (Li et al. 2015; Lu et al. 2015). In this paper, with the 80-day continuous microseismic monitoring data recorded in Qixing Coal Mine in China, we analyzed the distribution characteristics of the destructive seismic events with high released energy (rock bursts). By analyzing the evolution characteristics of microseismic events prior to the occurrence of rock bursts, a prediction model including four indicators was built. Then the conditional probability in probability theory was introduced as the assessment indicators to evaluate the prediction efficiency.

Microseismic monitoring system in Qixing Coal Mine

The Qixing Coal Mine belongs to Shuangyashan Mine Bureau of Longmei Group in China, which was put into operation in 1973. After the technological transformation, the annual designed production capacity was 2.4 million tons. There were 16 layers of coal in the field, the cumulative thickness was 21.5 m, of which 4, 6, and 8 coal seams were in the whole region, and the rest was locally recoverable. The Qixing Coal Mine was divided into two levels of mining, respectively −100 and −450 m.

The high-grade ordinary mining method was used and the annual mining velocity was about 600 m in the Qixing Coal Mine. The buried depth of the Dongsan working face was about 550 m, the coal thickness is about 2.45–3.60 m, and the mining direction of the working face was shown in Fig. 1. There were two large north-south trend faults in the mining areas, and there were several small faults found in the excavation process of the roadways. These small faults are mainly distributed in the four regions marked by A, B, C, and D in Fig. 1, respectively. The roof and floor of the coal seam are both sandstones, with a fine integrity in general except the local broken zones affected by faults.

As shown in Fig. 1, the real-time continuous microseismic monitoring was conducted during the mining process. There were nine high sensitivity sensors buried in the roadway to collect seismic waveforms. The sketch of the data acquisition system was shown in Fig. 2. The data acquisition modules (Paladin, Fig. 3a) were connected to the sensors (Fig. 3b),
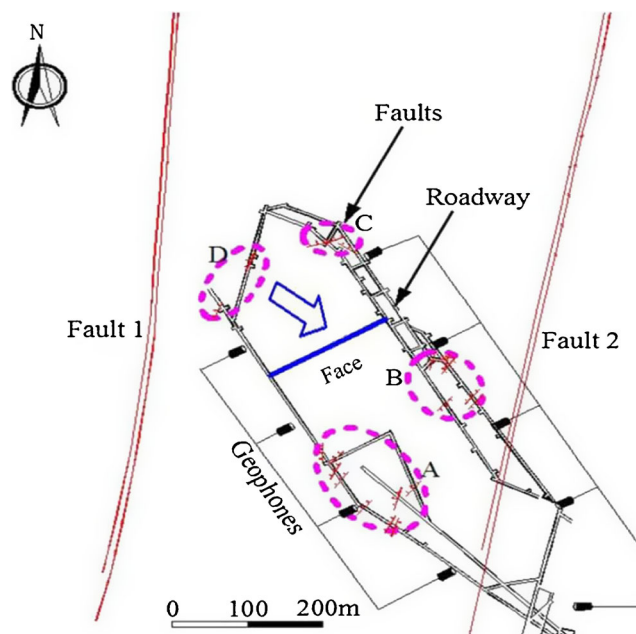

Fig. 1 The working face and the locations of seismic sensors

which converted the waveform signals into the high-resolution digital signals, and these signals were transmitted to the data processing center through the optical fiber cables in real time. Then, the microseismic events were detected and located in the processing center.

The association of rock bursts with active microseismicity and faults

The geological structures and stress distributions were not uniform during the mining process, which resulted in the uneven distribution of the rock burst risks in space. Here, we rely on analyzing microseismic events distribution in the mining
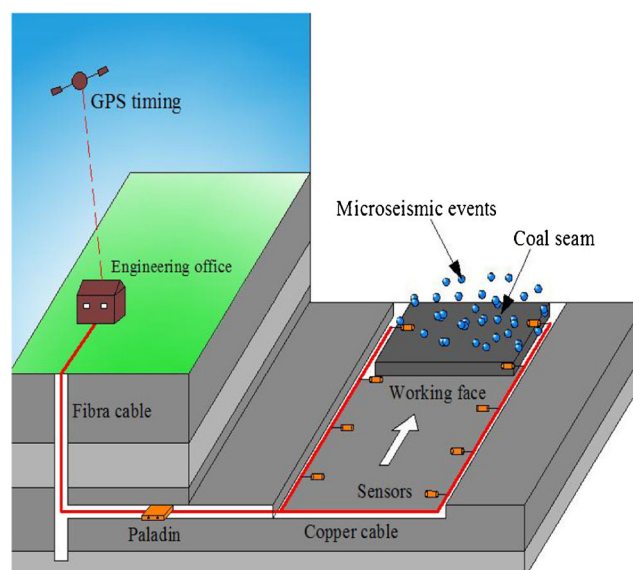

Fig. 2 The sketch of the data acquisition system

Fig. 3 The sensors and the data acquisition module (Paladin)

(a) Data acquisition module (Paladin)   (b) Sensors

process of rock bursts to delineate the high-risk zones for the early warning in mining.

Distribution characteristics of microseismic events

The spatial distribution of microseismic events detected and located by the monitoring system for about 80 days during the

mining process can be categorized into four stages (Fig. 4). With working face advancing, these microseismic events were mainly concentrated in three zones.

As shown in Fig. 4, for the first 40 days microseismic events were mostly concentrated in zone 1. Then, they were mostly clustered around zone 2 in the next 20 days while some microseismic events were clustered around zone 3 during the

Fig. 4 Distribution of microseismic events for different times during the 80-day monitoring period

(a) 20 days   (b) 40 days

(c) 60 days   (d) 80 days
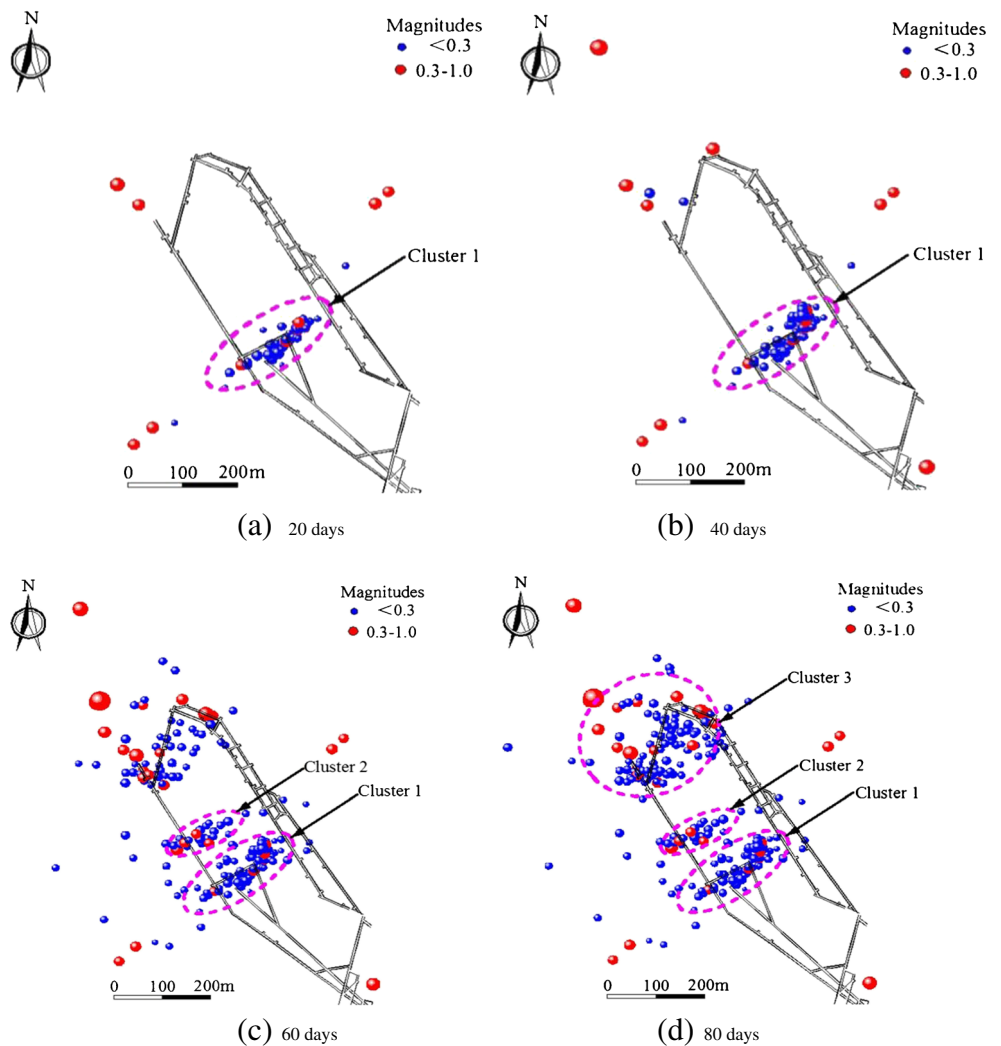
same time period. Finally, all the microseismic events in the last 20 days were located in the zone 3. Zone 1 is close to the zone 2 while there is big gap between zones 2 and 3. The seismic events with high released energy (i.e., rock bursts) were mainly located in these three zones. In each zone, the seismic events often occurred before the rock bursts, indicating the induced effect of the microseismic events by the rock bursts. Based on the relationships between microseismicity and rock bursts, we can hence delineate the rock burst high-risk zones by identifying active microseismic zones.

Influence of fault structures on the rock burst distribution

There are many complex factors that could induce rock bursts, among which the existence of faults has been proved to be a crucial one. Large strain energy can be accumulated around the faults due to the horizontal tectonic stress (Li et al., 2014). In the process of mining, the stress redistribution can easily activate faults (McKinnon, 2006); thus, the fault structures have a great influence on the spatial distribution of rock bursts. As shown in Fig. 5, some rock bursts concentrated in three zones are clearly linked to the existing small faults. In zone 1, there were a number of small faults (A, B in Fig. 5) detected in the adjacent roadways, inferring that there were some faults distributed between A and B. In addition, there were a number of rock bursts (zones 2 and 3 in Fig. 5) and the small faults overlapped (C, D in Fig. 5), which inferred that some rock bursts were caused by the fault activation.

In addition to microseismic locations, we can calculate source mechanisms by using the seismic waveforms (Šílený & Alexander, 2008). As shown in Fig. 5, the focal mechanism of an event located on fault F_1 suggested that the strike of
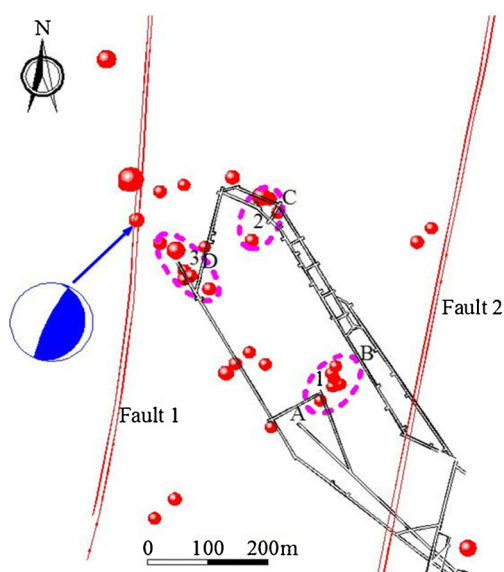

Fig. 5 Distribution of microseismic events (*red circles*) and the larger faults (*red lines*)

slipping surface followed the faulted structure trend, indicating that this event was induced by the activation of F_1. It can be seen that the stress redistribution in the mining process may induce the activation of the faults accompanied by rock bursts. Thus, the regions with faults often bear high risks of rock bursts. Through identifying the active microseismic zones and the existing faults, it can help delineate the high-risk zones of rock bursts, which are often associated with intensive microseismicity and are near existing faults. After identifying the high-risk zones, the supporting measures in these areas can be strengthened to avoid or reduce the occurrence of accidents. Beyond what has been stated, during the mining process, only a small shear microseismic event occurred in the fault F_1, and a large amount of strain microseismic events occurred in the mining surrounding rock. Compared with the latter, the occurrence probability of microseismic events in the fault F_1 is little; therefore, this paper mainly focus on the strain rock burst forecast in the mining surrounding rock.

Constructing and assessing rock burst prediction indicators

Constructing rock burst prediction indicators

The timely prediction of rock bursts is hard but essential; hence, it is necessary to comprehensively analyze the microseismic monitoring data to identify the precursors of rock bursts.

The average number N and the average released energy E

Rock bursts are the release of elastic waves in the process of deformation and failure of rock mass in high stress state while the stress evolution directly affects the microseismic activity. As shown in Fig. 6, the curves of the average number N and the average released energy E of microseismic events displayed the similar trend with time, which reflecting the microseismic activity at different stages.

It can be seen from Fig. 6a the whole monitoring curve could be divided into two periods while each period could be divided into three stages sequentially: the quiet stage (S_1), the active stage (S_2), and the transition stage of the microseismic activity (S_3). All these three stages (S_1, S_2, and S_3) corresponded to that of the stress evolution process respectively in the engineering rock mass, namely stress concentration stage, stress weakening stage, and stress transition stage. In the stress concentration stage, the accumulated stress did not yet reach the maximum strength of the rock mass, with few microseismic events occurrence. However, the stress accumulation had prepared for the increased microseismicity and released energy in the next stage. In the stress weakening stage, the local stress increased markedly and the rock mass
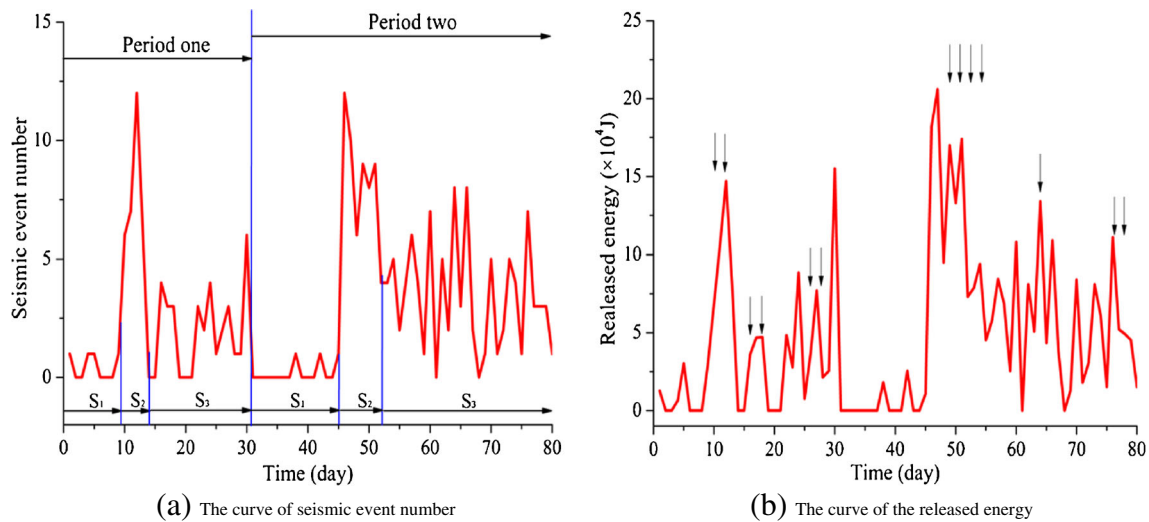
Fig. 6 The stages of the monitoring curves and the *arrows* mark the start of rock bursts

produced deformation and failure while the number of microseismic events increased sharply and remained at a high level during a certain time. After releasing the local concentrated stress, the curve entered the stress transition stage, i.e., the local high stress transferred to the near rock mass with a medium activity of microseismicity. A new period including the abovementioned three stages started after the energy fully released.

In the stress weakening stage and the beginning of stress transition stage, the local stress was so high that it tended to reach the maximum strength of the rock mass, often accompanied by high energy microseismic events, which pointed the direction of rock burst prediction. The occurrence times of the rock bursts were marked by arrows in Fig. 6b, which suggests that the day when the released energy reached the peak value and the subsequent 3 days had a high risk of rock bursts. Therefore, the sharp increasing of both the number of microseismic events and the released energy can be regarded as the precursors of rock bursts, i.e., the average seismic number N and average released energy E can be chosen as the prediction indicators of rock bursts.

The seismological parameter b and its decrease Δb

In seismology, the frequency and magnitude relations of the seismic events in a particular area often follow the formula:

$$\lg N = a - bM \tag{1}$$

where M indicates the magnitude of the seismic event, N indicates the number of earthquakes whose magnitude is M, a and b are regional parameters (Alvarez-Ramirez et al., 2012). This relationship has been widely applied in the prediction of earthquakes. The parameter b indicates the proportion of the seismic events with different magnitudes, reflecting the stress

level and rupture scale of the medium, is the capacity of hindering releasing energy of the rock mass (Yin et al., 1987).

As shown in Fig. 7, the b value tends to be decreasing in the whole process of microseismic monitoring which reflected the increase trend of large magnitude events. This also corresponded to the increase of the released energy, as seen in Fig. 6b. It is noted that the rock bursts often occurred after a sharp decrease of b value. Therefore, the decrease of b value compared to the previous day Δb can be chosen as one of the prediction indicators.

The potential maximum magnitude M_m

According to the seismicity absence theory, if the seismicity is always active in a particular area but a large magnitude earthquake did not occur in a certain time period, an earthquake may occur in the near future in this area. This theory is often
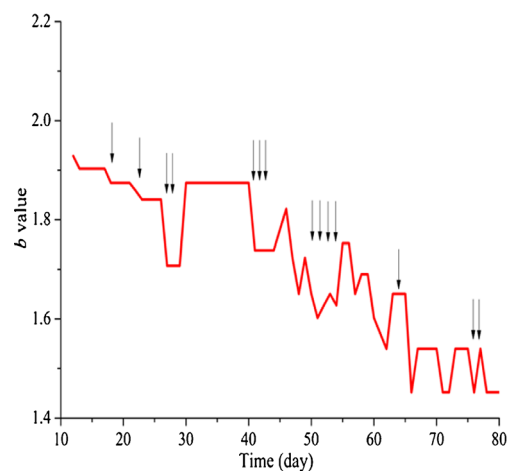

Fig. 7 The curve of the b value during the microseismic monitoring period

used in the prediction of tectonic earthquakes, which is also applicable in the microseismic prediction in the engineering scale.

There was an application of the theory in the working face in Qixing Coal Mine showed in Fig. 8. During the period of day 41 to 60, the microseismicity was active in the whole area A while the accumulated strain energy released through the seismic activity. While in the period of day 61 to 72, the seismic events occurred in the whole area except region B, in which the strain energy kept accumulating, indicating that the rock bursts might occur in this region. Entering the period of day 73 to 76, the microseismic events are mainly located in or near region B, besides some rock bursts occurred in the center of region B. Therefore, the local absence of seismicity can be regarded as a precursor of rock bursts.

In the Formula (1), when $N = 1$, $M_m = a/b$ indicates the potential maximum magnitude in the current magnitude distribution law. In the M-y coordinate system, it represents the intercept on the horizontal axis of a linear function $y = a-bM$, reflecting the capacity of creating a rock burst. Therefore, it is reasonable to choose M_m as a prediction indicator.

Assesing prediction indicators based on probability theory

Based on the recorded microseismic data, after selecting the appropriate alarm threshold, the alarm results of the four indicators were calculated in Fig. 9. It can be seen from Fig. 9, the successful prediction, i.e., the indicator exceeded the threshold value and the rock burst occurred in the same time had been identified. The graphs displayed that each indicator could predict some of the rock bursts, as well as miss other ones. To quantitatively evaluate prediction successful rate of various predictors, probability theory is introduced here. The conditional probability was chosen to assess the prediction efficiency of the indicators. Event A indicated that a seismic event larger than magnitude 0.3 (rock burst) occurred, B indicated

that the indicator exceeded the threshold and gave alarms, while $\overline{A}$ and $\overline{B}$ indicated their opposite states, respectively. There were four conditions in total:

(1) Positive successful prediction (AB): the prediction parameter exceeded the preset threshold and then gave the alarm before a rock burst. This was the case of an ideal prediction.

(2) Missing alarm (A$\overline{B}$)): the prediction indicator did not reach the threshold but a rock burst occurred in the absence of an alert. This situation showed a sudden rock burst without precursors, which was the main source of accidents.

(3) False alarm ($\overline{A}$B): the prediction model alarms did not find the occurrence of rock bursts. In this case, taking measures relying on the alarm result may lead to the delay of production and the waste of resources.

(4) Negative successful prediction ($\overline{AB}$): there was no warning or occurrence of rock bursts. In this case, no special measures should be taken.

The probabilities of the four mentioned conditions reflected the efficiency of the prediction results, which could be quantitatively assessed by the conditional probability as following:

P(B/A): it indicated the rate of forecasting the rock bursts successfully so the model should try to improve this value. P(A/B): it indicated the rate of effective warning, a model showed good efficiency when this value was high. $P(\overline{B}/A)$: $P(\overline{B}/A) = 1$-P(B/A), the missing alarm rate significantly affected the prediction effect. When it was high, a lot of rock bursts failed to be forecasted, including the risk of serious accidents. $P(\overline{A}/B)$: $P(\overline{A}/B) = 1$-P(A/B), the false alarm rate indicated the valid warning, having an important impact on the prediction efficiency. $P(A/B + \overline{B}/A)$: it indicated that the predicted results were consistent with the actual results. The
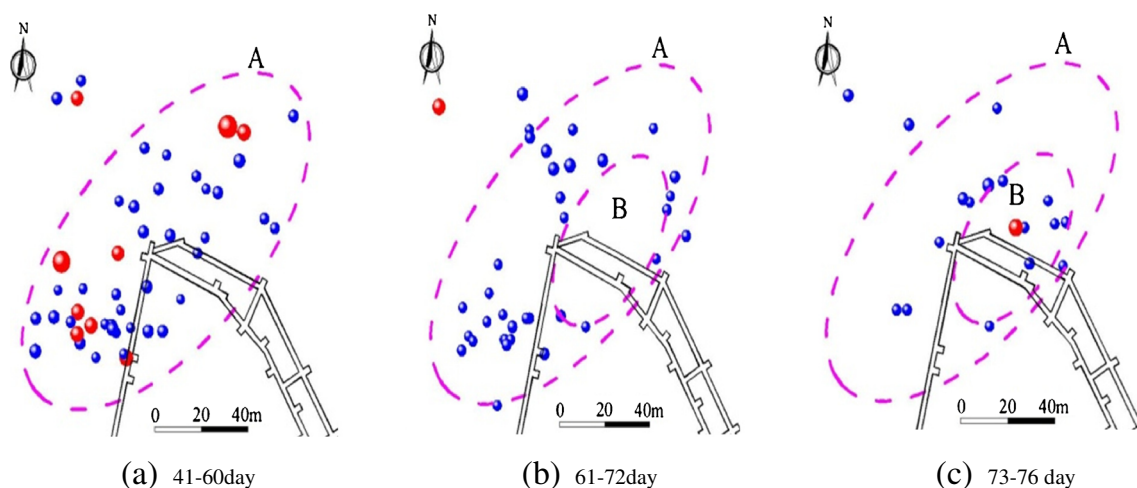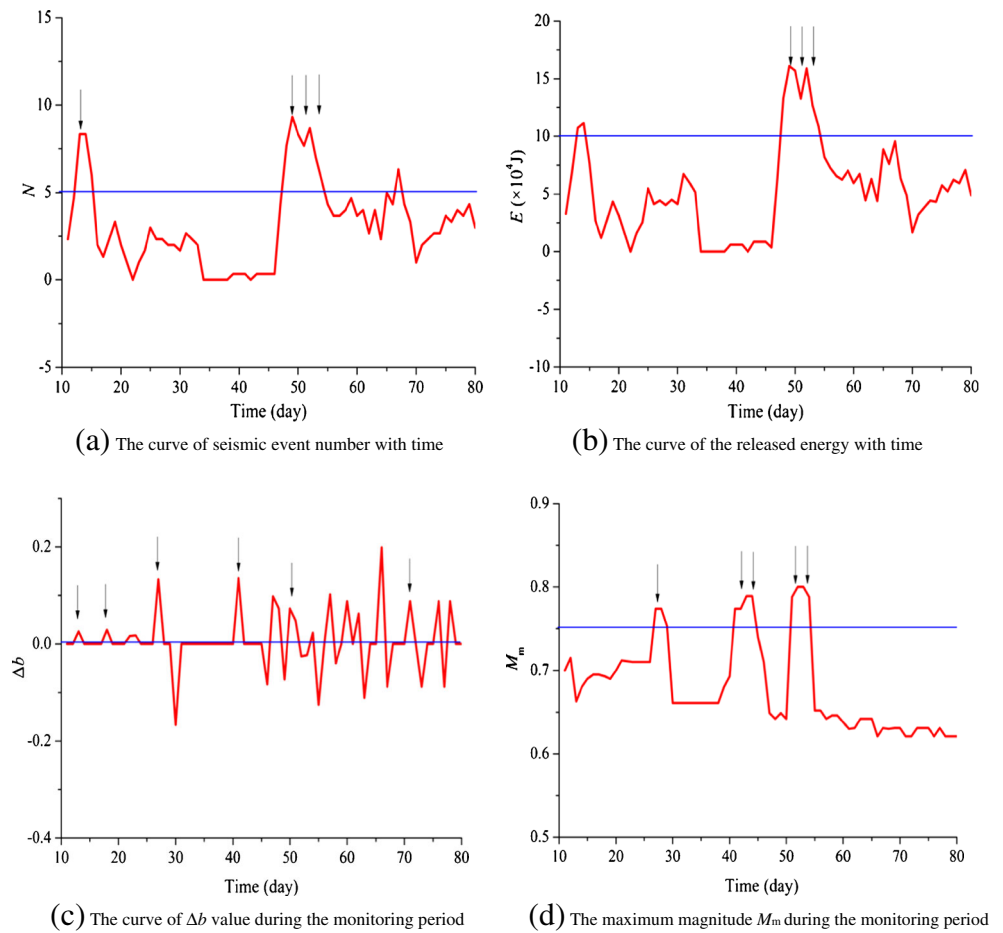

Fig. 8 Prediction of rock bursts using seismicity absence theory (Microseismicity is marked as *blue circles* and rock bursts are marked as *red stars*)

Fig. 9 Prediction efficiency of
the four indicators

(a) The curve of seismic event number with time

(b) The curve of the released energy with time

(c) The curve of Δb value during the monitoring period

(d) The maximum magnitude M_m during the monitoring period

prediction efficiencies of the above mentioned four indicators were listed in Table 1.

As seen from Table 1, we think that the probabilities of the prediction indicators are not less than 50% are good, so the probability 50% can be as a threshold value to evaluate the prediction efficiency of the prediction indicators. All the four indicators had prediction effect in different degrees, in which M_m performed best while Δb performed poor due to its high false alarm rate.

Discussions and conclusions

Sufficient and accurate information on geological, stress, and microseismic conditions is required for the development of reliable rock burst prediction models. In this paper, microseismic monitoring is used for the prediction of rock burst events and their location. It is shown that the accuracy of seismic events is one of the key issues, which depends primarily on the performance of the quality of the processing software and hardware of the

monitoring system, as well as the skills of the data processing analyst.

Based on collected microseismic data, a prediction model is developed, which includes the following main steps: analyzing the precursors, extracting the indicators, and determining the alarm thresholds. Microseismicity often shows similar characteristics before a rock burst. To quantitatively describe the precursory characteristics, it is essential to extract accurate prediction indicators that have a solid physical basis. For example, the "b" value chosen in this paper is widely used in seismology to describe the seismic magnitude distribution and its physical meaning engineering scale is thoroughly discussed, making itself a reasonable indicator. Secondly,

Table 1 Prediction efficiency of the four indicators

Name	P(B/A)	P(A/B)	P($\overline{B}$/A)	P($\overline{A}$/B)	P(A/B + $\overline{B}$/$\overline{A}$)
N	0.37	0.50	0.63	0.50	0.73
E	0.32	0.55	0.68	0.45	0.74
Δb	0.63	0.39	0.37	0.61	0.63
M_m	0.53	0.71	0.47	0.29	0.81

these quantitative indicators must be calculated automatically because the monitoring is continuous and lasts for a long time. Finally, the chosen thresholds significantly affect the model efficiency; hence, it is necessary to continuously train and optimize the threshold values in an established model.

Four indicators are extracted from the microseismic data to predict rock burst risks, including the average number of microseismic events N, the average energy released E, the decrease Δb of the seismological parameter b, and the potential maximum seismic magnitude M_m. To quantitatively compare the performance of these four prediction indicators, a number of rock bursts are assessed using conditional probabilities. The results show that all four indicators well predict rock bursts and the prediction indicator using the potential maximum seismic magnitude M_m appears to be the best.

The prediction model in this paper relies only on microseismic monitoring data. By using other types of data such as mining-induced stress, it is possible to derive better prediction models. However, this would increase the complexity of the prediction model.

References

Alvarez-Ramirez J, Echeverria JC, Ortiz-Cruz A, Hernandez E (2012) Temporal and spatial variations of seismicity scaling behavior in Southern Mexico. J Geodyn 54:1–12. doi:10.1016/j.jog.2011.09.001

Driad-Lebeau L, Lahaie F, Heib MA, Josien JP, Bigarre P, Noirel JF (2005) Seismic and geotechnical investigations following a rockburst in a complex French mining district. Int J Coal Geol 64: 66–78. doi:10.1016/j.coal.2005.03.017

Husen S, Kissling E, Deschwanden AV (2013) Induced seismicity during the construction of the Gotthard Base Tunnel, Switzerland: hypocenter locations and source dimensions. J Seismol 17:63–81. doi:10.1007/s10950-011-9261-8

Jiang YD, Pan YS, Jiang FX, Dou LM, Ju Y (2014) State of the art review on mechanism and prevention of coal bumps in China. J China Coal Soc 39(2):205–213. doi:10.13225/j.cnki.jccs.2013.0024

Lesniak A, Isakow Z (2009) Space-time clustering of seismic events and hazard assessment in the Zabrze-Bielszowice coal mine, Poland. Int J Rock Mech Min Sci 46:918–928. doi:10.1016/j.ijrmms.2008.12.003

Li JR, Song B, Cui JY (2015) Seismic dynamic damage characteristics of vertical and batter pile-supported wharf structure systems. Journal of Engineering Science and Technology Review 8(5):180–189. doi:10.14006/j.jzjgxb.2016.07.019

Li SG, Lv JG, Jiang YD, Jiang WZ (2014) Coal bump inducing rule by dip angles of thrust fault. Journal of Mining & Safety Engineering 31(6):869–875

Lu JT, Yang ND, Ye JF, Liu XG, Mahmood N (2015) Connectionism strategy for industrial accident-oriented emergency decision-making: a simulation study on PCS model. International Journal of Simulation Modelling 14(4):633–646. doi:10.2507/IJSIMM14(4)6.315

Ma TH, Tang CA, Tang LX, Zhang WD, Wang L (2016) Mechanism of rock burst forcasting based on micro-seismic monitoring technology. Chin J Rock Mech Eng 25(3):470–483. doi:10.13722/j.cnki.jrme.2014.1083

Mansurov VA (2001) Prediction of rockbursts by analysis of induced seismicity data. Int J Rock Mech Min Sci 38:893–901. doi:10.1016/S1365-1609(01)00055-7

McKinnon SD (2006) Triggering of seismicity remote from active mining excavations. Rock Mech Rock Eng 39(3):255–279. doi:10.1007/s00603-005-0072-5

Pastén D, Estay R, Comte D, Vallejos J (2015) Multifractal analysis in mining microseismicity and its application to seismic hazard in mine. Int J Rock Mech Min Sci 78:74–78. doi:10.1016/j.ijrmms.2015.04.020

Šílený J, Milev A (2008) Source mechanism of mining induced seismic events—resolution of double couple and non double couple models. Tectonophysics 456:3–15. doi:10.1016/j.tecto.2006.09.021

Xia YX, Kang LJ, Qi QX, Mao DB, Ren Y, Lan H, Pan JF (2010) Five indexes of microseismic and their applications in rock burst forecast. J China Coal Soc 35(12):2011–2016

Yin XC, Li SY, Li H, Wang M (1987) On the physical essence of b value for AE of rock tests and natural earthquakes in terms of fracture mechanics. Acta Seismol Sin 9(4):364–374. doi:10.1007/BF02652408

Yu Q, Tang CA, Li LC, Li H, Cheng GW (2014) Nucleation process of rockbursts based on microseismic monitoring of deep-buried tunnels for Jinping II Hydropower Station. Chinese Journal of Geotechnical Engineering 36(12):2315–2322. doi:10.11779/CJGE201412021

Yuan RF, Li HM, Li HZ (2012) Distribution of microseismic signal and discrimination of portentous information of pillar type rockburst. Chin J Rock Mech Eng 31(1):80–85

Zhao YX, Jiang YD, Wang T, Gao F, Xie ST (2012) Features of microseismic events and precursors of rock burst in underground coal mining with hard roof. J China Coal Soc 37(12):1960–1966